Chapter

Long-Term Changes in Sea Surface Temperature Off the Coast of Central California and Monterey Bay from 1920 to 2014: Are They Commensurate?

Laurence C. Breaker

Abstract

We examine to what extent the waters of Monterey Bay act independently of those along the central California coast. Sea surface temperatures (SSTs) from 1920 to 2014 from the central California coast and Monterey Bay were analyzed for long-term trends. To estimate the trends, singular spectrum analysis and empirical mode decomposition were employed. Between 1920 and 1940, long-term trends inside and outside Monterey Bay revealed rapidly increasing temperatures. After 1940 trends inside the bay indicate that temperatures increased from ~1950 for the next 40 years, peaking around 1990, and then decreased rapidly through 2013. Offshore, temperatures increased to the early 1960s, after which they decreased until 2014. El Nino episodes, the Pacific decadal oscillation (PDO), and increased coastal upwelling contribute to the long-term trends. Also, the impact of regime shifts associated with the PDO may be sustained for decades. Overall, the differences in the trends inside and outside Monterey Bay are significant only during summer where large-scale processes dominate offshore, and smaller-scale processes are important in and around the bay. Finally, our results suggest that waters inside the bay, although they co-vary with the waters further offshore, often appear to behave independently based on the long-term trends.

Keywords: long-term trends, nonlinear trends, singular spectrum analysis, ensemble empirical mode decomposition, central California coast, Monterey Bay, El Nino, Pacific decadal oscillation, coastal upwelling, regime shifts

1. Part I: background and preliminaries

1.1 Introduction

This study seeks to determine if the waters off the central California coast and Monterey Bay have warmed significantly during the 94-year period from 1920 to 2014 by examining sea surface temperatures (SSTs) inside the bay and outside the bay off the central California coast. The period of observation was terminated in December 2013 due to the unexpected arrival of a massive temperature anomaly

off the coast of central California called the "Blob" in early 2014 [1]. We also seek to determine if warming inside the bay differs from warming outside the bay. This comparison is motivated, in part, by the following question. Is the bay merely an extension of the waters further offshore along the central California coast and thus expected to have similar physical properties, or are there local processes within or near the bay that significantly alter those properties? One of the arguments that favors the similarity of these waters is due to the relatively large entrance of the bay compared to its longest internal dimension (approximately 36 vs. 42 km). Thus, the waters offshore have wide and direct access to the bay. Also, residence times in the bay are not overly long, on the order of 7 days [2]. Thus, there is relatively less time for local waters that enter the bay to be modified before they exit. Early work in the greater Monterey Bay area by Skogsberg [3] and Skogsberg and Phelps [4], for example, tended to favor similarity. However, several of the more recent process-oriented studies that have been conducted on finer temporal and spatial scales in or near the bay would favor dissimilarity [5, 6]. In the simplest case, if we were to find significant differences in the long-term trends of temperature inside and outside the bay, we might favor dissimilarity.

To make these determinations, we calculate the long-term trends in SST in both domains. The results depend to a certain degree on how we distinguish between "coastal" waters and waters further offshore and on the methods that are used to estimate these trends. In this study we examine not only the long-term trends but also the nature of the processes that most likely have contributed to the trends.

The coastal ocean off central California and Monterey Bay is strongly affected by the process of coastal upwelling. According to Garcia-Reyes and Largier [7], coastal upwelling off central and northern California occurs from April through June, followed by relaxation of the upwelling-favorable winds from July through September. During the winter months from December through February, extratropical storms occur which contribute to cooler surface temperatures through wind mixing and the transfer of sensible and latent heat. Other times of the year tend to be transitional.

Based on the work of Mendelssohn and Schwing [8] and Garcia-Reyes and Largier [9], coastal upwelling off central California has been shown to have increased over the past several decades. According to Bakun [10] and Snyder et al. [11], coastal upwelling may be expected to increase in the future due to climate change or long-term climate variability.

Coastal upwelling is not the only physical process in the California Current System (CCS) that has a significant impact on SST. Ocean fronts, Ekman pumping, eddies, and squirts and jets all affect temperature. With respect to ocean fronts, the front that separates upwelled waters near the coast from oceanic waters further offshore is a primary example [12]. Positive wind stress curl off the central California coast during the spring and summer leads to Ekman pumping or offshore upwelling due to Ekman divergence. This is an important process that brings colder waters to the surface away from the influence of a coastal boundary. Both cyclonic and anticyclonic eddies are found in the CCS. Cyclonic eddies promote upwelling and are often found south of capes along the California coast. A major anticyclonic eddy is occasionally observed just west of Monterey Bay [13]. Jets and squirts occur off central and northern California characterized by patterns of vigorous circulation, readily observed in satellite images of SST [14].

During the spring and summer, upwelled waters are found inside Monterey Bay that often originate at Pt. Ano Nuevo (**Figure 1**), are advected down the coast, and then enter the bay forming a cyclonic pattern of circulation that has frequently been observed [15, 16]. In addition to upwelled waters that are advected into the bay from further offshore, local upwelling occurs in northern Monterey Bay due to the diurnal sea breeze that is well developed during the summer [5].

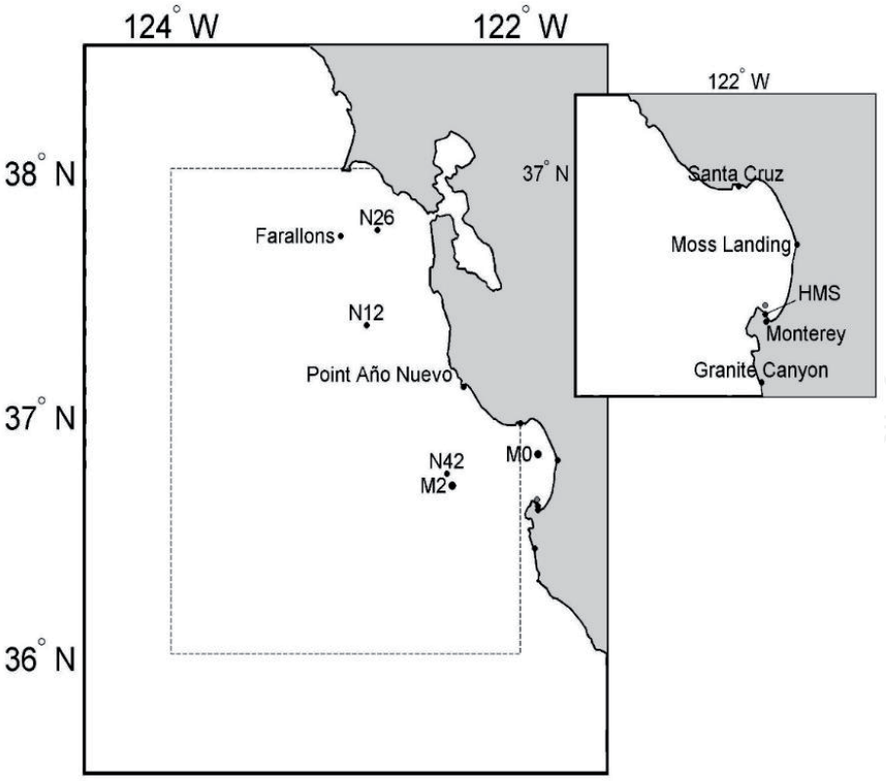

Figure 1.
*A map of the study areas including the offshore domain shown by the dotted box and the inshore domain which is Monterey Bay. The location where the data used to evaluate the SST from HMS is shown in the inset by the gray dot just above (north) of the Hopkins Marine Station (HMS). N26, N12, and N42 refer to National Data Buoy Center (NDBC) buoy locations (***Figure 4***).*

Now we turn to a review of the previous work that is directly relevant to this study. Inside Monterey Bay, SSTs from the Hopkins Marine Station at the southern end of the bay (**Figure 1**) have been examined on several occasions for possible long-term trends [17–19]. The record begins in 1919 and extends up to the present time. In each case, warming rates of approximately +0.01°C/year were found, based on linear, least-squares fits to the data.

Barry et al. [17] found that the annual maximum in SST increased more rapidly than the annual minimum. Further, they observed that changes in the flora and fauna of the intertidal zone in Monterey Bay coincided with well-documented secular warming along the US West Coast. In addition, they indicated that climate-related faunal changes in California's rocky intertidal community were related to long-term changes in the coastal environment based on the SST data from Hopkins and inferred that these changes were due to climate warming.

Sagarin et al. [18] indicated that temperature changes in Monterey Bay tended to be monotonic when the Hopkins record was subdivided into selected time periods between 1920 and 1995. They also concluded that climate warming, based on the Hopkins record and other sources, was responsible for range-related shifts in the intertidal communities along the California coast.

In a previous study, Breaker [19] examined the record at Hopkins for the period from 1920 to 2001 and also estimated the long-term linear trend. He found the slope to be +0.011°C/year, consistent with the values obtained by Barry et al. and Sagarin et al. He further found that the trend was statistically significant at the 95% level of confidence. Breaker examined the seasonal effects on long-term warming and found that warming in July exceeded the yearly rate by ~7%, whereas warming in

January was less than the yearly rate by almost 19%, consistent with the results of Barry et al. [17]. In the same study, Breaker also estimated the relative importance of the various processes that contributed to variability in the data and found that the annual cycle and its first harmonic, El Nino warming episodes, the Pacific decadal oscillation (PDO), and the long-term trend were all significant sources of variability.

The present study departs significantly from the previous study in a number of ways. First, one of the questions from the earlier work that was left unanswered was to what extent did the results from Monterey Bay reflect what was happening on larger scales outside the bay. Second, the record is now almost 15 years longer than the record used by Breaker [19], and significant cooling has occurred during this period. Third, in the previous study, only the long-term *linear* trend was calculated, and, since then, it has become clear that using a linear basis to model long-term changes in the data is a poor choice. Finally, we apply singular spectrum analysis to the data together with empirical mode decomposition to obtain independent estimates of the long-term trends. The methods are complementary and provide a basis for evaluating their quality.

Off the coast of central California between 35°N and 39°N, Garcia-Reyes and Largier [9] examined long-term trends in SST and several related parameters from the existing network of NDBC buoys for the period from 1982 to 2008. During the period of observation, the upwelling-favorable alongshore winds increased and SST decreased, consistent with increased coastal upwelling. Not only was the upwelling stronger, the length of the upwelling season was found to have increased, starting earlier in the spring and ending later in the fall. Relevant to this study, the observed trend in SST was found to be strongest off central California. Further, the observed cooling was limited to coastal waters over the shelf, where upwelling is the dominant process during the spring and summer. Because the record was only 27 years long, it was not possible to determine if the apparent trends were related to decadal or longer-term periodic behavior.

A larger view of the CCS was taken by Field et al. [20] who examined long-term warming from extensive records of SST off California and from other regions of the North Pacific. Much of their data spanned the twentieth century although it did not resolve the region of coastal upwelling off California. For locations where SSTs were examined in the North Pacific, the Pacific decadal oscillation (PDO) index accounted for a significant fraction of the observed variability. Also, near-surface temperature variations throughout the CCS were found to be similar between regions. Their data indicate that from 1900 on, strong negative SST anomalies prevailed during the period leading up to the early 1920s. They resulted from higher atmospheric pressure off California that intensified flow in the California Current and upwelling during this period. During the twentieth century, data from the CCS revealed warming trends with slopes ranging from +0.007°C/year to +0.010°C/year, similar to the warming observed in Monterey Bay over approximately the same period. Also, the negative anomalies in the early years of the twentieth century have contributed significantly to the positive trends that have been observed in records that are long enough to include this period.

Finally, we return to the original question posed in the title of this chapter. Although the word "commensurate" can refer to many different measures of similarity, we take it to mean to what extent do the waters inside Monterey Bay co-vary with the waters outside the bay with respect to their physical properties. During the winter the influence of the poleward flowing Davidson Current dominates the behavior of waters inside and outside the bay, and thus SSTs are generally similar [13]. During the summer when coastal upwelling is a dominant process, the relationship between the waters inside and outside the bay becomes more complicated

because smaller-scale processes in and around Monterey Bay become important. Thus, the answer to this question may depend to a significant degree on the season, with higher co-variability to be expected during the winter than during the summer. Our subsequent analyses will shed more light on this question.

1.2 Data sources

1.2.1 Data sources inside the bay

The primary source of SST data inside the bay comes from the Hopkins Marine Station (HMS) located at the southern end of Monterey Bay in Pacific Grove (**Figure 1**). The data have been acquired nominally at 08:00 am PST on a daily basis since January 20, 1919. Because of several issues that have affected data quality over its duration, Breaker et al. [21] reconstructed the record by making time-of-day adjustments for varying data collection times, removed gaps, improved data resolution consistency, and, finally, reconstructed one entire year (1940) that was missing from the record based on regression with daily SSTs from the Farallon Islands. For the purposes of this study, we have extracted the 95+-year period from January 1920 through May 2015 although most of the results we present are limited to the period from 1920 through 2013 to avoid the confounding effects of the major temperature anomaly that arrived in early 2014. The daily observations were then averaged to obtain monthly mean values. Because these data have been acquired at a single location, they represent point observations. Daily observations of SST adjacent to HMS were also collected from August 1, 2006, through January 31, 2007, to ascertain the representativeness of the data from Hopkins per se and are discussed in Section 3.

1.2.2 Data outside the bay

The primary source of data for the 2°× 2° region shown in **Figure 1** along the coast of central California is the International Comprehensive Ocean-Atmosphere Data Set (ICOADS). These data were provided by the NOAA/OAR/ESRL PSD, Boulder, Colorado, USA, from their web site at http://www.esrl.noaa.gov/psd/. Monthly averaged SSTs were acquired for the region from 36 to 38°N, and from 122 to 124°W, for the period from January 1920 through May of 2015. Again, most of the results we present are limited to the period that ends in December 2013. These monthly data represent spatially averaged values and as a result are inherently different than the point observations we employ inside the bay.

Figure 2 shows the number of observations per month in the 2 × 2 degree study area starting January 1920. Overall, the number of observations remains below 1500 per month until 2004 when a significant increase occurs. The inset shows the period from 1920 through 1970 where the numbers of observations are far smaller.

Plots of the monthly averaged SST data from the Hopkins Marine Station, inside Monterey Bay, and from ICOADS, adjacent to the central California coast, outside the bay, are shown in **Figure 3**. Superimposed on the data are smoothed versions shown in red obtained using a *LOWESS* smoothing function. The method is nonparametric and performs robust, locally weighted regression. It fits linear or quadratic basis functions to the data at the center of neighborhoods where the radius of each neighborhood contains a specific percentage of the data points. This type of smoothing function does not lose degrees of freedom at the ends of the record and introduces minimal distortion at these locations. The fraction of data in each neighborhood, and thus the smoothness, is determined by two parameters, the degree of the local polynomial basis function (linear or quadratic), λ, and the level

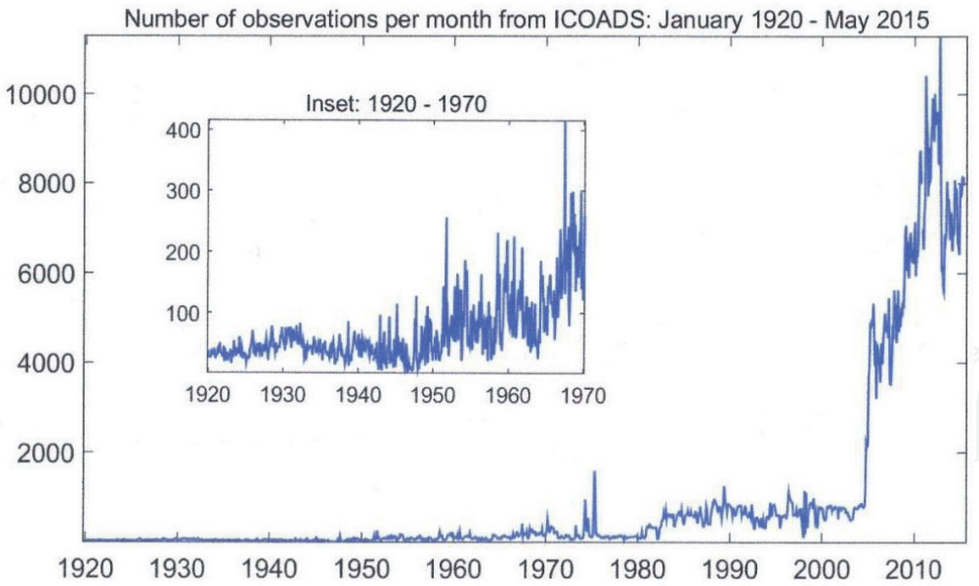

Figure 2.
The number of observations per month from ICOADS for the offshore domain are plotted by month since 1920. The inset shows the period between 1920 and 1970 where the number of observations per month is relatively small.

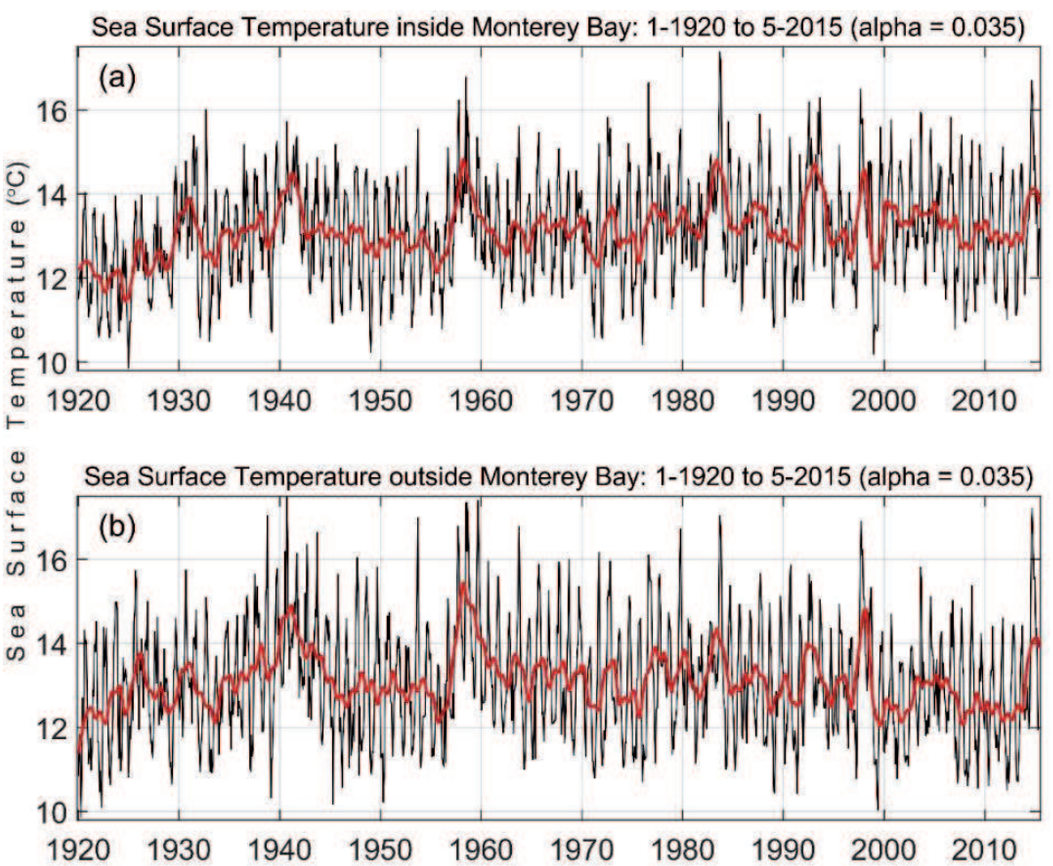

Figure 3.
Sea surface temperature from HMS inside Monterey Bay (a), and from ICOADS, off the coast of central California, outside the bay (b). The red curves provide smoothed versions of the data where important features such as major El Nino warning episodes can be more easily identified.

of smoothing, α. In the present study, the degree of the local polynomial has been set to quadratic. The smoothing parameter is specified by the choice of α, where $0 \leq \alpha \leq 1$. For α equal to 0, no smoothing occurs, and for α equal to 1, we obtain

essentially a straight line. The goal is to choose α large enough to obtain as much smoothness as possible without distorting underlying patterns in the data [22].

At the level of detail shown in **Figure 3**, the relative importance of the annual cycle is readily apparent. It is also possible to identify major El Nino warming episodes that occurred in 1931–1932, 1940–1941, 1958–1959, 1982–1983, 1986, 1992–1993, and 1997–1998. In this study we usually refer to El Nino warming events or simply El Ninos rather than ENSO which has a broader meaning that includes La Nina cooling events as well. Off central and northern California, it is the warming phase of the El Nino phenomenon that stands out and not the cooling phase.

Also, as mentioned earlier, there was a major increase in SST that is readily apparent in the data inside and outside the bay during 2014. We show it here but do not include it in our calculations. According to **Figure 3**, the increase in SST based on the unsmoothed data during 2014 clearly exceeds 3°C, somewhat larger than the reported value of 2.5°C [1].

1.3 Data representativeness

Inside the bay, the SST data are acquired at the shoreline in a somewhat sheltered area next to the Hopkins Marine Station. Next to the coast where the circulation is expected to be weaker, residence times could be longer, leading to increased temperatures, locally. To examine this question which has arisen before, we compared the SST data from HMS with SSTs acquired at an adjacent offshore location. Specifically, daily SSTs at HMS were compared with daily SSTs acquired just offshore, slightly north of HMS in southern Monterey Bay (**Figure 1**). The data were acquired over a period of almost 6 months from August 4, 2007, through January 31, 2008. This data was acquired specifically to evaluate the daily observations of SST that have been collected at HMS (M. Denny, personal communication). The two data sets are almost identical with a mean difference of less than 0.1°C over the 6-month period of observation. Based on an earlier comparison of SST data between HMS and Santa Cruz, located at the north end of Monterey Bay (**Figure 1**), Breaker [19] concluded that the data from HMS was generally representative of SST data collected elsewhere in the bay, consistent with the results presented here.

The offshore data used in this study have been acquired over a spatial domain that is regional in scale (**Figure 1**). The number of observations per month has increased significantly since 1920 (**Figure 2**). This, in turn, changes the uncertainty in estimating the monthly means over the length of record. This problem is not unique in climate research. The globally averaged record of surface air temperature used extensively in climate studies suffers from the same problem.

Spatial biases in the SST observations acquired over the offshore domain lead to biases in the monthly mean values that are calculated. This arises for at least two reasons. First, the observations that enter into the monthly means are not uniformly spaced over the region since they come from a variety of sources. Second, even if the observations were acquired uniformly, the underlying ocean itself is not thermally homogeneous. The second factor becomes particularly apparent during the spring and summer when coastal upwelling occurs. During this period SSTs may increase by 5°C or more between the coast and the offshore boundary of the study domain. These biases are significantly reduced between November and February during the Davidson Current period when the waters tend to become more isothermal. Overall, spatial biases are to be expected, they vary with the season, and they will influence the trends we calculate.

To examine the spatial bias problem we have drawn from Garcia-Reyes and Largier [9] who examined SST and other data for the period from 1982 through 2008

from eleven NDBC Environmental Data Buoys along the California coast. Three of those buoys (N26, N12, and N42) are located in our offshore study area (**Figure 1**). They calculated the linear trends in SST for the upwelling season which they defined as the period from March through July for all buoys. We have taken our offshore data, with the buoy data specifically removed, and calculated the linear trend for the same time period and upwelling season (**Figure 4**). For buoys N26, N12, and N42, Garcia-Reyes and Largier obtained slopes of −0.032, −0.034, and −0.021°C/year, respectively, with a mean of −0.0290°C/year, taken over the three buoys. Based on our data, we obtained a slope of −0.024°C/year, slightly less than, but still relatively close to, the value obtained by Garcia-Reyes and Largier. If the non-buoy data were randomly spaced over the domain, we would find this result encouraging in that it suggests a certain degree of spatial homogeneity in the data. If, however, the non-buoy data were concentrated closer to the coast, as we suspect, then all we have shown is that the buoy and non-buoy data tend to be consistent.

1.4 Long-term trends

1.4.1 Background

Although trends may appear to be intuitively obvious, precise definitions are hard to find. According to Fuller [23], the term "trend" only acquires meaning when a specific procedure is used for its estimation. For time series, trends have been labeled as deterministic when the trend per se is modeled explicitly [24]. A trend implies non-stationarity of the first order, and so its removal may transform the data into a stationary process. Linear trends are often fitted to the data, but as we shall see in the present study, the long-term changes we observe are not linear. In this regard, two studies are relevant. Jevrejeva et al. [25] analyzed sea level data for long-term trends that were nonlinear in nature using a variation of singular spectrum analysis (SSA) called Monte Carlo SSA. This method provides error estimates associated with the trend as well. Breaker et al. [26] examined sea surface temperature data from the coast of Ecuador for long-term trends that were inherently nonlinear using ensemble

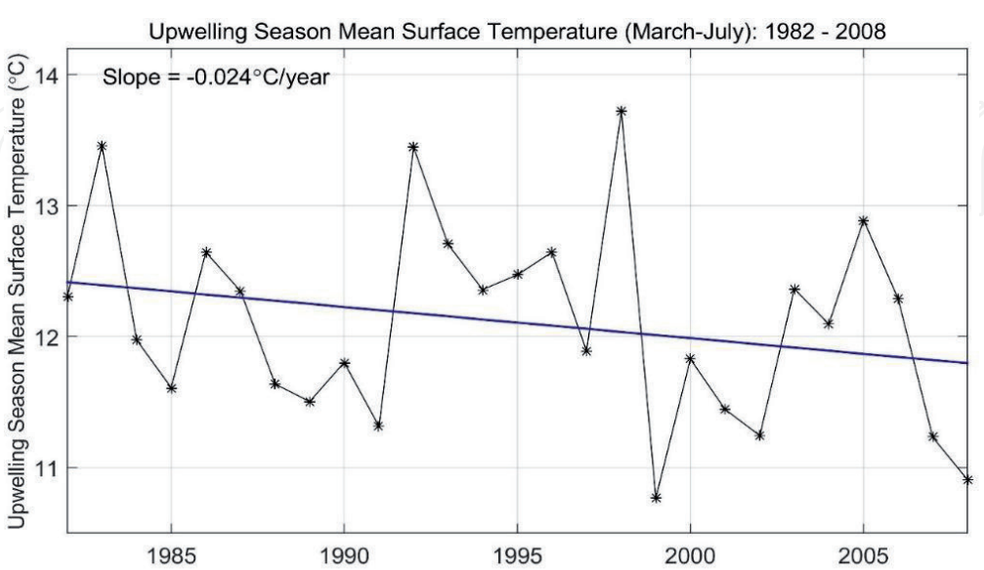

Figure 4.
Mean seasonal SST for the offshore domain for the upwelling period from March through July plotted on a yearly basis for 1982 through 2008. A least-squares linear fit to this data yields a slope of −0.024°C/year.

empirical mode decomposition. This method performed well in extracting the long-term trends regardless of the degree to which the data tended to be nonlinear.

In our experience, when the data are trend-dominant, different methods of estimating the trend often yield similar results, but when the trend is not a dominant feature in the data, then different methods may yield significantly different results. One common definition of the trend is that of a smoothly varying function whose first derivative does not change sign [27]. Although this definition may be intuitively appealing, in practice, it is often too restrictive. Although formal definitions of the trend are scarce, Wu et al. [28] recently proposed the following: "The trend is an intrinsically fitted monotonic function or a function in which there can be, at most, one extremum within a given data span." For rather extensive reviews of methods for estimating trends, see Esterby [27] and Alexandrov et al. [29].

1.4.2 Methods

To estimate long-term trends in the data, we use two methods of spectral decomposition, singular spectrum analysis (SSA) and ensemble empirical mode decomposition (EEMD). We find that SSA and EEMD are often complementary in the trends they produce, and, when they are, it increases our confidence that meaningful trends have indeed been extracted from the data. Both methods decompose the data into a set of independent modes. To this extent, the methods are similar. However, the methodologies per se are entirely different. We give a brief introduction to each method here and the appropriate references.

Singular spectrum analysis (SSA) decomposes a time series into a set of independent modes, similar in many respects to principal component analysis. The method is well-suited for analyzing data that are nonstationary and/or nonlinear due to the adaptive nature of the basis functions employed. A lagged covariance matrix (a Toeplitz matrix, in this case) is formed from the time series that is decomposed into eigenvalues, eigenvectors, and principal components. Reconstructed components can be calculated from the eigenvectors and principal components that represent partial time series whose sum over all modes reproduces the original time series. These components, modes, or eigentriples as they are variously called are often amenable to physical interpretation. The number of modes that is selected is called the window length and determines the resolution of the decomposition. The mode or modes that correspond to the trend can often be selected by inspection when the trend contains a significant portion of the variance, but when the trend is relatively weak, the problem becomes more difficult. Alexandrov [30] provides a new approach for extracting the trend when it is not a dominant feature in the data. In this study, the trend, although not the most dominant feature in the data, is robust enough that we do not resort to the method of Alexandrov in order to isolate it. Finally, we note that because the method of decomposition in SSA is global in nature, problems can arise at the boundaries of the data. For further details concerning SSA, see [31–35].

Empirical mode decomposition (EMD) is a method of decomposing a time series into a sequence of empirically orthogonal intrinsic mode function (IMF) components and a residual. In EMD, the number of modes is determined by the data, whereas in SSA, the number of modes is a free parameter that must be specified by the user. Like SSA, EMD is data adaptive and well-suited for the analysis of nonstationary and nonlinear time series. The IMF components are often physically meaningful because the characteristic scales in each case are determined by the data itself. As in SSA, selected modes may require grouping in order to extract a physical basis. Each IMF represents a mode of oscillation with time-dependent amplitude

and frequencies that lie within a specific band of frequencies, the center of which defines the mean period of that mode. The process of extracting the individual modes or essential scales from the data is called sifting and is performed many times to produce a single IMF. In practice, extracting the trend may require that not only the residual but one or several of the highest adjacent modes be grouped in order to reconstruct it.

One problem in the application of EMD in the past was that mode mixing often occurred when a time series included intermittently occurring signals with widely separated time scales. To address this problem, EMD now includes a noise-assisted component in its calculation. Wu and Huang [36] developed the technique that is now called "ensemble EMD," or EEMD, which defines the true IMF as the mean of an ensemble of IMFs and, in the process, preserves the physical uniqueness of the decomposition. An ensemble member consists of the signal plus white noise of finite amplitude. The magnitude of the white noise that should be added is given by the ratio of the standard deviation of the first IMF to the standard deviation of the data itself and is called N_{std}. Although this is the recommended value, in many cases, if slightly different values above or below the recommended value are used, the resulting IMF patterns remain stable although the patterns can differ slightly. Typically, the number of realizations or ensemble size is several hundred in order to generate the ensemble. The ensemble size that we have used in this study is 300. Thus, in EEMD there are two free parameters that must be specified, the level of white noise to be added and the ensemble size. The problem of end effects is discussed in Wu and Huang [36]. In the latest version, the IMFs themselves are extended after they are calculated which helps to reduce problems at the boundaries. The problem is further reduced in the noise-assisted version, i.e., in EEMD, because the slopes of the IMFs tend to be more uniformly distributed in the ensemble. For more information concerning EMD and EEMD, see [36–40].

2. Part II: analyses, results, and discussion

2.1 Analyses

2.1.1 Application of SSA and EEMD

In applying SSA to the data inside and outside the bay, the decomposition was accomplished using a window length, L, of 240 months inside the bay, and L = 316 months in the offshore domain (outside the bay). Although we started with L = 240 months in the second case, due to the occasionally encountered problem of mode mixing (the partial presence of one mode in an adjacent mode), we increased L in steps to its present value in order to suppress it. In SSA terminology this issue is referred to as the separability problem and is addressed in detail in Golyandina et al. [32]. **Figure 5** shows the first 12 reconstructed modes for L = 316 outside the bay. The first two modes (Ro1 and Ro2) correspond to the annual cycle, and modes 6 and 7 (Ro6 and Ro7) correspond to the first harmonic. Harmonic components in the data often appear as matched pairs in the reconstructed modes where the amplitudes and phases are the same or similar [41], making it easier to identify them. Finally, we note that mode 5 is trend-like in nature.

Inside the bay, the corresponding SSA decomposition indicates that modes 1 and 2 correspond to the annual cycle and modes 9 and 10 to its first harmonic (not shown). In this case, mode 3 is trend-like and reveals two maxima, one in the early 1940s and the second around 1990, reminiscent of the maxima that we associate with the Pacific decadal oscillation (PDO). At this point, we tentatively associate

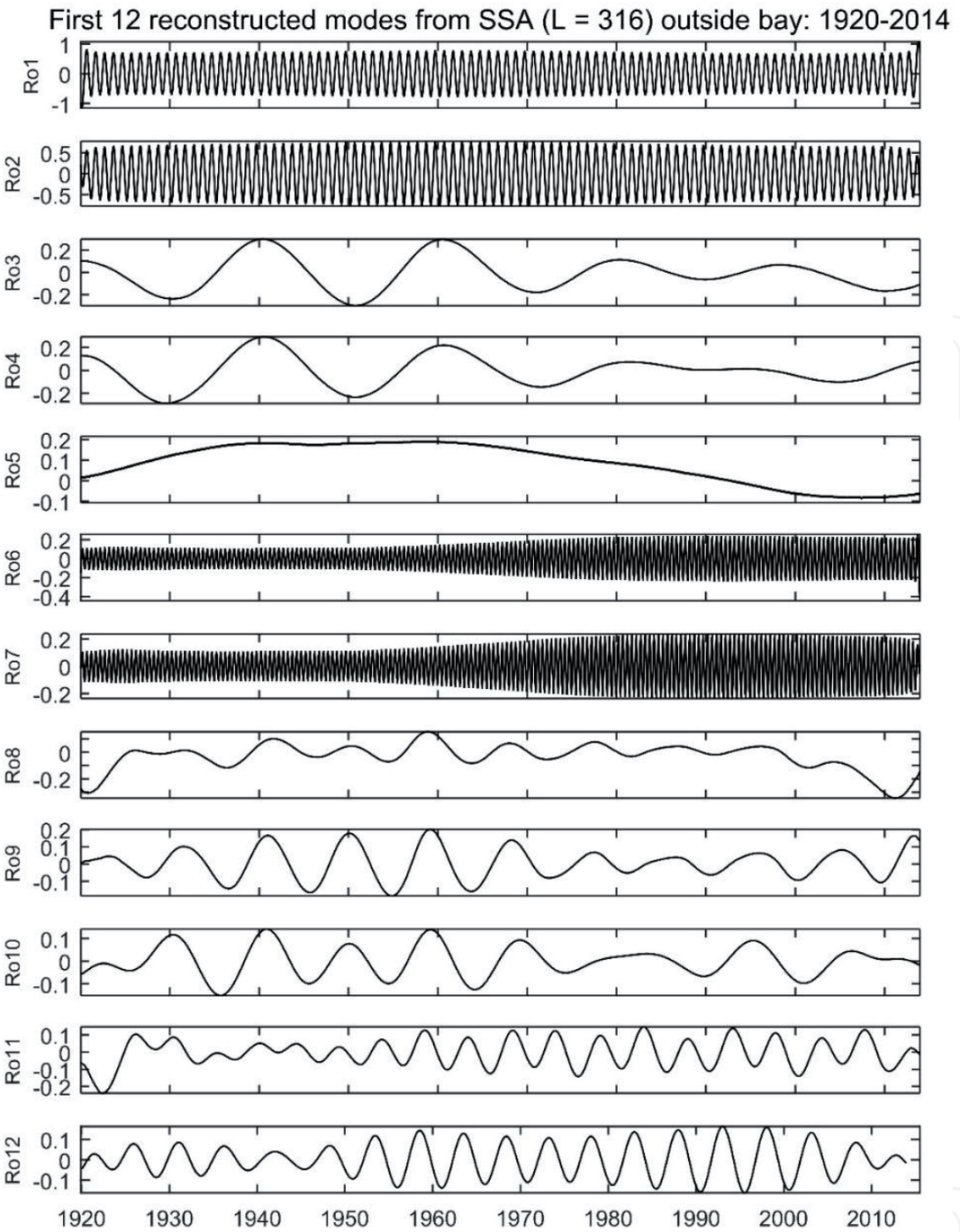

Figure 5.
The first 12 reconstructed modes are shown from the SSA decomposition of the data (L = 316) outside the bay. The first two modes show the annual cycle, and modes 6 and 7 show the first harmonic of the annual cycle. Reconstructed mode 5 shows the long-term trend.

this mode and mode 5 from the decomposition outside the bay with the underlying trends, awaiting the results from the EEMD decompositions.

In decomposing the data inside the bay based on EEMD, the noise parameter, N_{std}, was determined to be 0.33 and the ensemble size was 300. The EEMD decomposition produced 10 modes (imf1 – imf10) where imf10 is often referred to as the residual. In a similar decomposition of the data outside the bay, the value for N_{std} was 0.31 with the same ensemble size, and, again, 10 modes were produced. The results from inside the bay (black) for all 10 modes are shown in **Figure 6**, together with the three highest modes (imf8, imf9, imf10—blue) from outside the Bay. The results obtained inside and outside the Bay are generally similar except for the

highest three modes, and thus the reason why they are included in the same figure. Also, it is these modes that most likely contribute to the long-term trends.

Next, we calculate and plot the variances for each mode inside and outside the bay from the EEMD decompositions (**Figure 7**). If we can identify the oceanic processes in accordance with the modal decompositions, then we may be able to estimate their relative importance. The estimated center frequencies for each mode (i.e., band) and location are given in **Table 1**. The center frequencies are not fixed because they are determined by the data and so vary slightly between locations [42]. The variances tend to be similar overall between locations but there are several notable differences. The variances associated with the first modes are similar

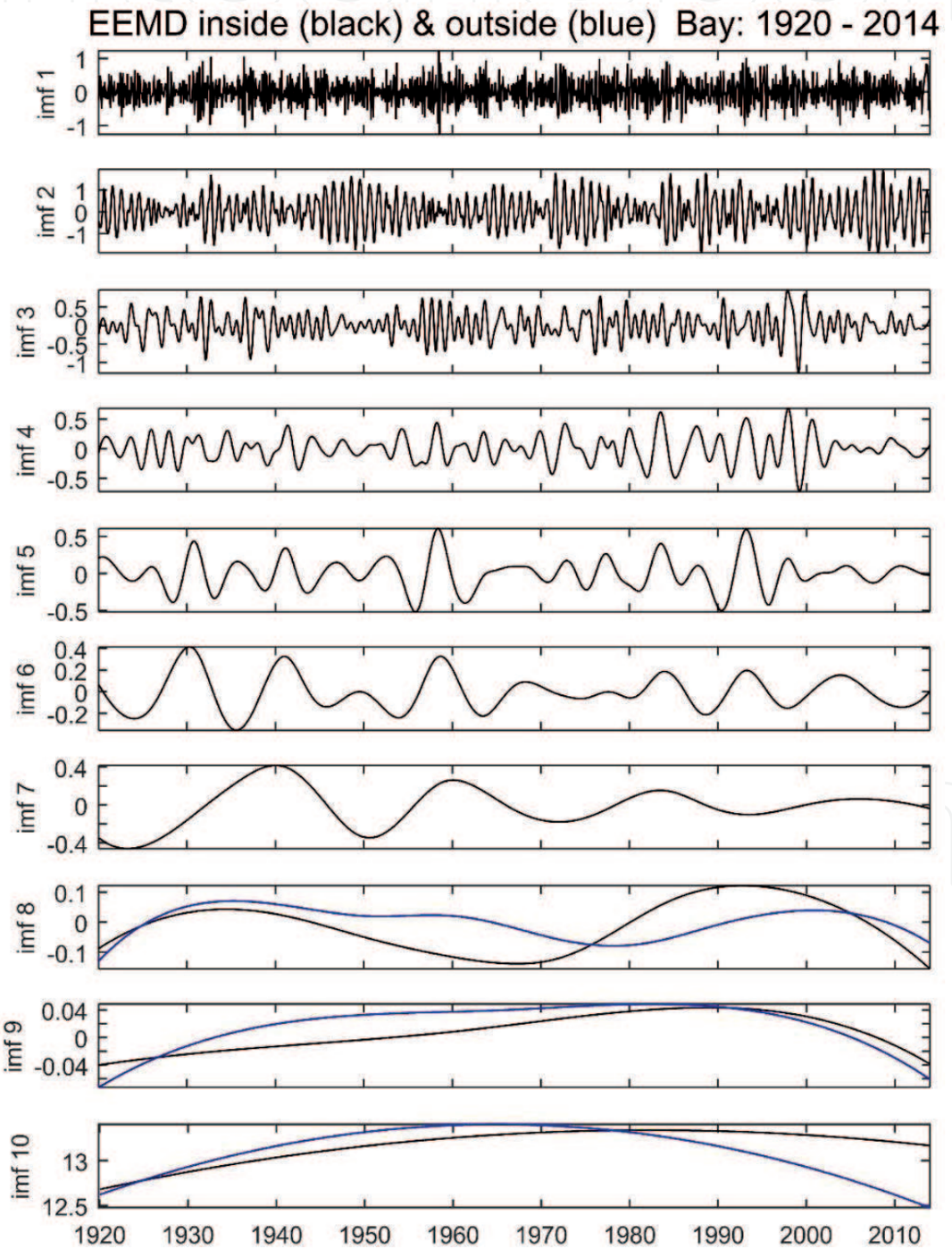

Figure 6.
EEMD decompositions of SST from inside and outside Monterey Bay each generated 10 modes. All 10 modes are shown for inside the bay (black) and the highest 3 modes (imf8 – imf10) are shown for outside the bay (blue) as well. See the text for details.

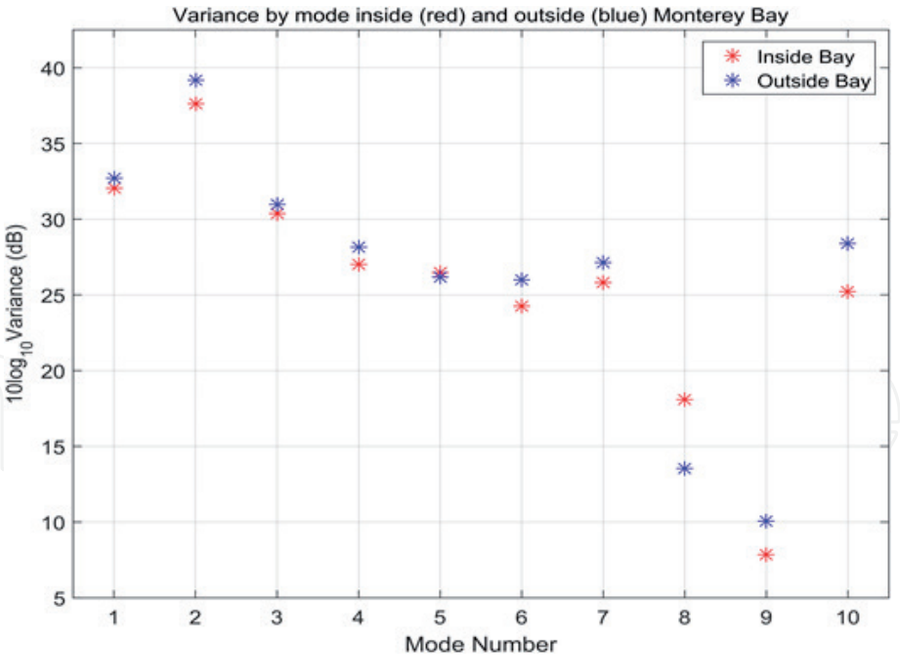

Figure 7.
Variances by mode obtained from the EEMD decompositions for observations acquired inside the bay (red) and outside the bay (blue).

IMF mode number	Inside bay	Outside bay	Comments
1	3.13 (3.8 months)	3.95 (3.0 months)	
2	1.0 (1.0 year)	1.0 (1.0 year)	
3	0.55 (1.8 years)	0.55 (1.8 years)	Depends on smoothing
4	0.31 (3.2 years)	0.328 (3.0 years)	
5	0.17 (5.9 years)	0.16 (6.3 years)	
6	0.082 (12.2 years)	0.06 (16.7 years)	
7	0.047 (21.3 years)	0.036 (27.8 years)	
8	0.012 (83.3 years)	0.012 (83.3 years)	
9	—	—	Insufficient data
10	—	—	Insufficient data

Table 1.
Approximate center frequencies in cycles per year and the corresponding periods in months or years (in parentheses) for each mode from the EEMD decompositions.

and represent approximately 15% of the total variances. The primary periods are 3 months outside and 3.8 months inside the bay with most of the variability distributed over a band that extends from roughly 2– 6 months. A significant portion of the variability in this range should be related to coastal upwelling and upwelling-related processes such as offshore Ekman transport and the evolution of ocean fronts, eddies, jets, and squirts [43]. The second modes correspond primarily to the annual cycle and in both cases represent over 50% of the total variance. Modes 3 and 4 are transitional in nature in that they generally fall between the periods we associate with annual and interannual variability (**Figure 6**). By mode 5, interannual variability is dominant with the major El Ninos of 1957–1958, 1982–1983, 1992–1993, and 1997–1998 making their appearances at both locations. Modes 6–8 show a gradual transition from what are distinctly El Nino events (mode 6) to

a signature that we associate with the Pacific decadal oscillation (PDO) in mode 8, in each case. The PDO index [44] characteristically has a maximum circa 1940 and a second maximum circa 1990 that are separated by a period of approximately 50 years (**Figure 12**). Of particular note, the variance associated with the PDO in mode 8 is far greater inside the bay than it is outside the bay (by at least 6 decibels which corresponds to a factor of 2). We discuss this curious result in more detail in the final section of the text. Mode 9 in both cases carries very little variance but could be related to the long-term trend. The residual long-term trends are shown in mode 10. Finally, the variance associated with the residual long-term trend outside the bay far exceeds that of the trend inside bay as shown (**Figure 6**).

2.1.2 Trend identification

The highest and the next two highest modes from EEMD inside and outside the bay are shown in **Figure 8a** and **b**. In more detail, the highest mode (imf10), the sum of modes 9 and 10 (imf9 + imf10), and the sum of modes 8, 9, and 10 (imf8 + imf9 + imf10) are shown inside (**Figure 8a**) and outside (**Figure 8b**) the bay. First, we note that the results of adding modes 9 and 10 together (i.e., imf8 + imf9—red) makes little difference, as expected, based on the small variance carried by mode 9. It is not until we include mode 8 (i.e., imf8 + imf9 + imf10—green) that we introduce more structure into the trends. We note that the added structure is primarily due to the inclusion of the PDO in our tentative definition of the long-term trend.

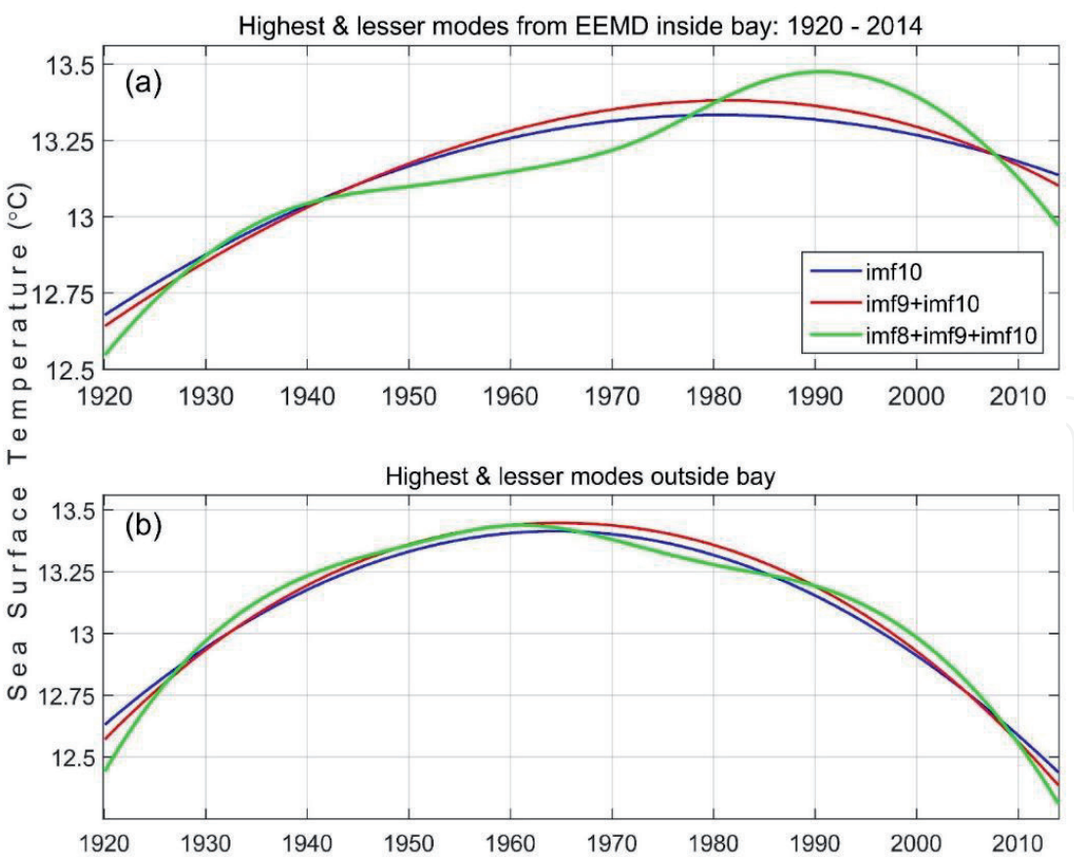

Figure 8.
In the upper panel (a), the highest mode (imf10—blue), the sum of the highest and next highest modes (imf9 + imf10—red), and the sum of highest, next highest, and third from the highest modes (imf8 + imf9 + imf10—green) are shown from the EEMD decomposition of the data from outside the bay. In the lower panel (b), the same combinations of modes from the EEMD decomposition of the data from inside the bay are shown.

The SSA results, however, provide a slightly different story. In deciding which mode or combination of modes corresponds to the long-term trend, the similarity between the tentatively identified SSA trends and the EEMD-derived trends obtained by combining modes 8, 9, and 10 becomes apparent. The trends from SSA and EEMD inside the bay are shown in **Figure 9a** and those trends outside the bay in **Figure 9b**. A high degree of similarity between SSA and EEMD is quite apparent inside the bay but to a lesser extent outside the bay.

Differences in the trends outside the bay can be explained, at least in part, by two factors. First, it was necessary to employ a larger value for the window length in the SSA decomposition outside the bay (L = 316 vs. 240 months) because of mode mixing that resulted in greater smoothing and thus a reduction in amplitude. The second problem relates to end effects. In our experience, SSA does not perform as well as EEMD when it comes to resolving structure near the beginning and end of the modal time histories. According to Mann [45], the problem of how to smooth data with trends near boundaries is particularly problematic. As stated earlier, SSA can exhibit problems at the boundaries of the reconstructed modes, but the boundary issues associated with EEMD, in our experience, are far smaller. Also, because the methods we have used are completely independent, there is no reason to expect that the combinations of modes which we choose to call the trend in one case should be the same or even similar in the other.

In summary, we favor the trends obtained from EEMD primarily because the problem of mode mixing that arose in the SSA decomposition outside the bay led to an unrealistic reduction in the amplitude of the reconstructed mode. Secondly, the end effects from EEMD are expected to be smaller than they are from SSA, and that has been our experience. It is important to note, however, that SSA has been most helpful in guiding our selection of the modes from EEMD to include or group in arriving at our definition of the long-term trends.

2.1.3 The trends per se

Based on the EEMD results, the trends inside and outside the bay are shown together in **Figure 9c**. They are clearly nonlinear and would be poorly approximated using a linear basis. During the 1920s the trends in SST are similar, but by 1930, the trends start to diverge with SSTs increasing more rapidly offshore than inside the bay. This pattern of divergence continues until about 1960 when SSTs inside the bay start to increase more rapidly and SSTs offshore start to decrease. Opposing trends in SST since 1960 continue for approximately the next 30 years. By about 1990, however, the trend inside the bay changes from increasing to decreasing temperatures, consistent with strongly decreasing temperatures offshore. Without the arrival of the warm anomaly in early 2014, both trends would most likely have continued to reflect decreasing temperatures up through at least 2014 and perhaps for several years longer.

2.1.4 Uncertainty

Uncertainty in climate science has been referred to as a "monster," a "wicked problem," or "the 800 pound gorilla who is sitting in the next chair" [46]. Mathematically, estimating uncertainty is considered to be an ill-posed problem because different methods of estimating this quantity often produce different results.

In our work, the question of uncertainty in estimating the trends shown in **Figure 10** naturally arises. As stated by Moore et al. [47] regarding nonlinear trends, we expect the confidence interval of a nonlinear trend to be significantly smaller than it would be for a least-squares fit to the same data, since the data are

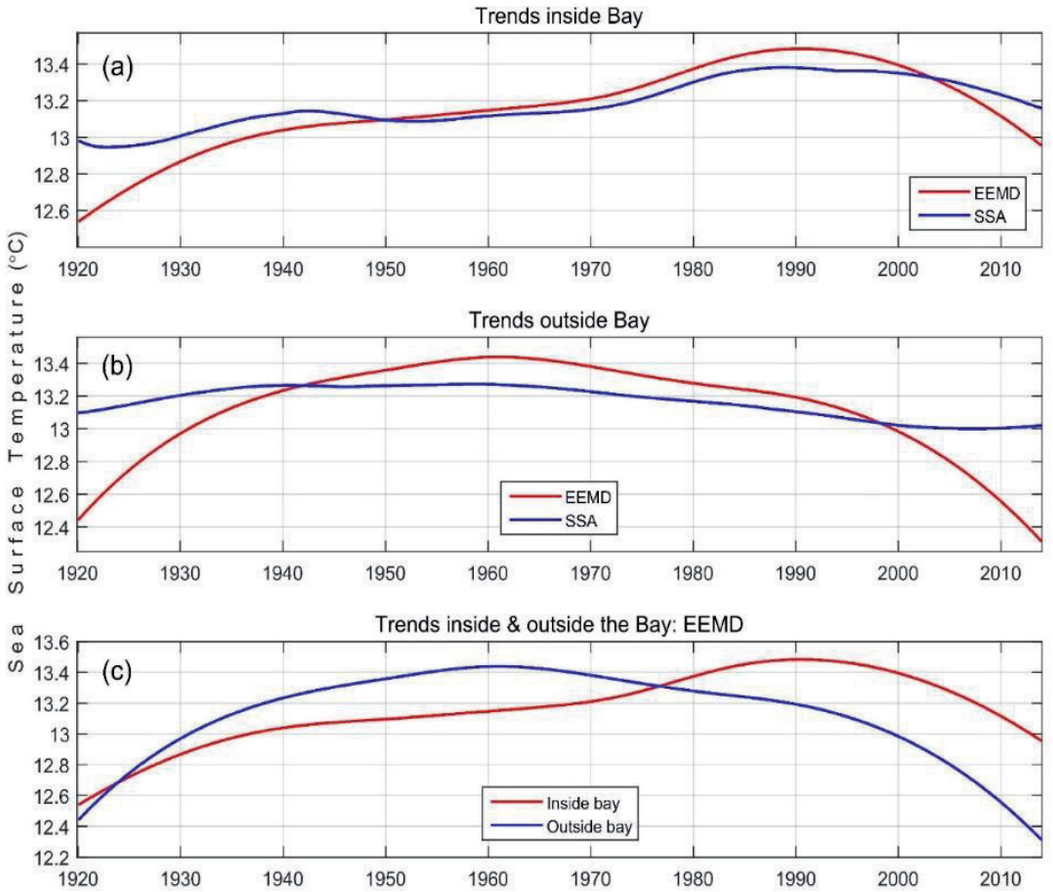

Figure 9.
The trends obtained from SSA (blue) and EEMD (red) of the data from inside the bay are shown in (a). The trends obtained from the data outside the bay using the same color convention are shown in (b). (c) shows the trends inside (red) and outside (blue) the bay together based on the results of EEMD.

not forced to fit any specified basis function. However, they acknowledge that it is not necessarily a simple problem to estimate uncertainty in nonlinear cases. In our case, since we have two independent estimates of the trends, the spread between them does provide at least a rudimentary estimate of the uncertainty if we assume that the true trend lies between the two estimated trends. Of course, we could also use a weighted average to reflect our greater confidence in the results from EEMD, but how to determine such weights is anything but clear. To proceed with equal weighting, one could go even further and assume that the two curves in each case correspond to ±1 standard deviation about the mean of a Gaussian distribution and, from that point, calculate the 95% confidence intervals. This approach is used in small sample theory in statistics when no other information is available (personal communication, Prof. David S. Crosby). This approach has the distinct advantage of using both estimates of the trend to estimate a confidence interval that would be associated with the expected value of the two trends obtained by calculating their mean.

We have proceeded to calculate confidence intervals for the trends inside and outside the bay. The results are shown in **Figure 10a** and **b**. There are several ways these intervals can be estimated. In this case, the differences between the trends and the mean values between them serve as a proxy for the standard deviations. We can calculate a global standard deviation for each record and use that estimate to obtain the 95% confidence intervals following the usual assumptions and tables given in any standard text on statistics. However, this approach yields confidence intervals that are constant over the entire record. A better approach in our view is to consider the proxy values locally and to calculate the 95% confidence intervals separately for each

time point. This has the distinct advantage of emphasizing the increased uncertainty that arises at the end of each record at the price of indicating no uncertainty where the records intersect, a feature that is unrealistic. We also obtain the expected result that the uncertainty increases or decreases where the differences between the two records increase or decrease. Finally, we return to the question raised in Section 1.3 concerning the differences between the point observations acquired inside the bay, and the area-averaged observations acquired offshore. Although the uncertainties we have obtained address this question to some degree, simulations from an ocean model would be better-suited to address this question in detail.

2.2 Ocean processes and time scales

2.2.1 Seasonal variability

The modal patterns we have already observed are inherently smooth because they contain only the highest modes from the various EEMD decompositions. To examine the underlying processes that contribute to these patterns in more detail, we have stratified the data from inside and outside the bay by season where we define the summer season as the mean of June, July, and August and the winter season as the mean of November, December, and January. We have smoothed the results slightly using LOWESS for added clarity.

In **Figure 11a**, inside the bay (red) during summer, the patterns are strongly positive and are almost identical for the first two decades indicating that the process or

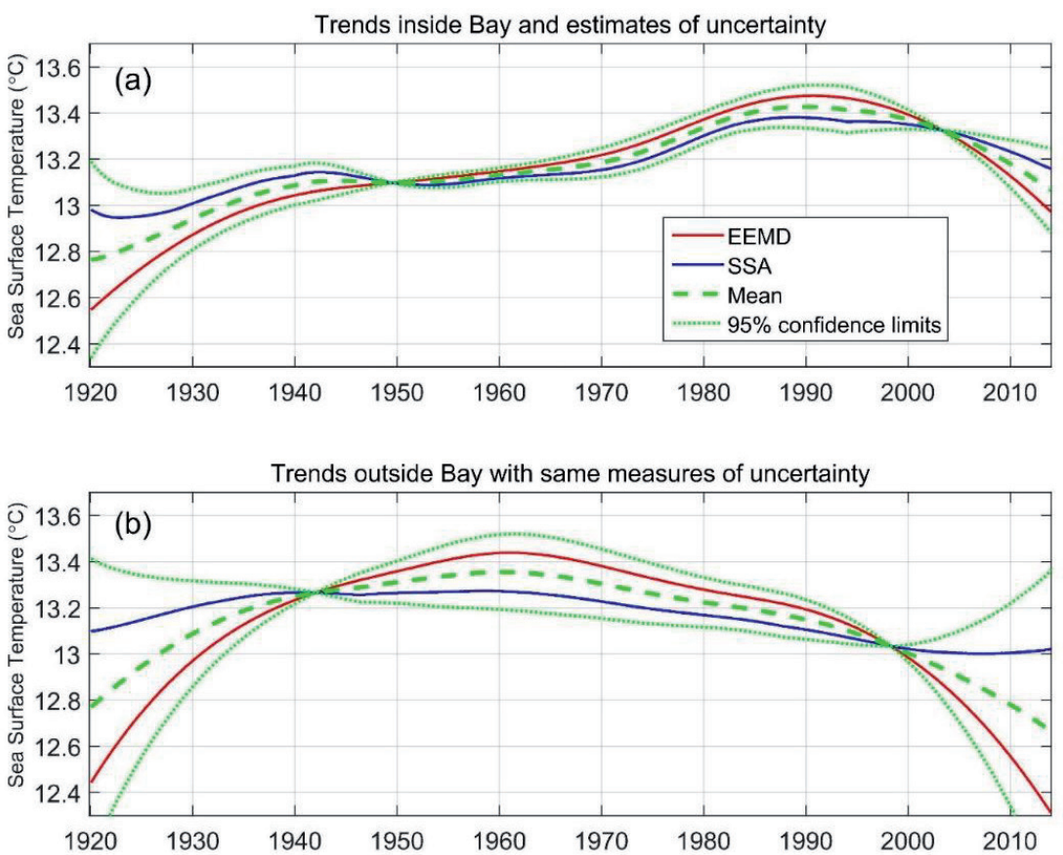

Figure 10.
The upper panel (a) shows the SSA- and EEMD-derived trends inside Monterey Bay together with one measure of uncertainty. The green dashed line shows the estimated true trend based on the mean of the SSA and EEMD trends. The green dotted lines show the 95% confidence intervals about the mean. In the lower panel (b), the original trends, the estimated mean value, and the 95% confidence intervals are again shown but, in this case, for the waters outside the bay.

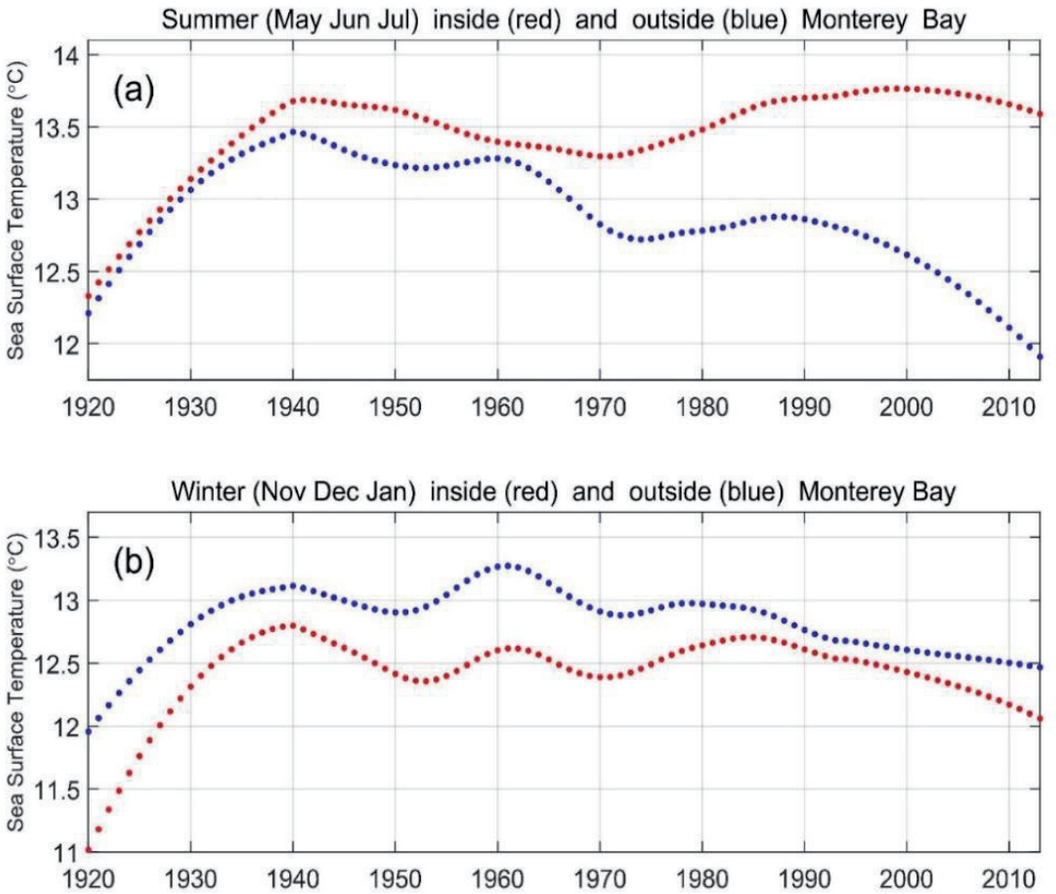

Figure 11.
In both panels, the data have been stratified by season where summer corresponds to the average of May, June, and July and winter corresponds to the average of November, December, and January. In the upper panel (a), the data for summer inside (red) and outside (blue) the bay are shown. In the lower panel (b), the data for winter inside (red) and outside (blue) the bay are shown. LOWESS smoothing has been applied in each case with the degree of smoothing (alpha) set equal to 0.35 (see text for details). Finally, the points have not been connected to emphasize the fact that they represent seasonal values, and so the curves that are plotted are not continuous functions.

processes responsible for contributing to the rapid warming included both domains. The rates of increase in temperature during this period approach 5°C/100 years! After 1940, these trend-like patterns moderate and gradually diverge, and by 2014 they have diverged to a point where bay waters are almost 1.5°C warmer than waters outside the bay. These patterns convey a more detailed picture of the variability that could not be observed in the original trends.

Continuing, inside the bay, although SSTs increased by over 1°C by 1940, between 1940 and the early 1970s, they actually decreased. The increase now occurs mainly between the early 1970s up to ~2000, after which they decrease until 2014. Outside the bay, SSTs actually decrease, albeit with significant variations along the way, until the end of the record (December 2013). Although the overriding pattern is downward, after the early 1970s, SSTs increase slightly until the late 1980s, after which they decrease rapidly, consistent with our previous observations.

Four points of note are as follows: (1) the patterns of rapidly increasing SST during the first two decades inside and outside the bay were almost identical, indicating that the warming process was a truly dominant phenomenon during that period; (2) SSTs actually decrease from 1940 to the early 1970s inside the bay; (3) cooling, for the most part, occurred outside the bay starting ~1940 (vs. ~1960) and continued until the end of the record; and (4) surface temperatures inside the bay were significantly higher than outside the bay during the summer, especially over the last 20 years or so.

In **Figure 11b**, during the winter, the patterns inside (red) and outside (blue) the bay are, to a high degree, similar, even with the higher resolution. However, although the patterns are similar, the temperatures outside the bay reflect SSTs that are roughly 0.2–1°C higher during winter. In more detail, maxima in temperature occur at both locations circa 1940 and during the early 1960s. These maxima co-occur with El Nino warming episodes with the addition of the co-occurrence of the first major maximum in the PDO index in or about 1940 (**Figure 12**).

What is common in all cases is the very rapid rates of warming during the first 20 years of each record and the slightly less rapid rates of cooling during the last 20 years or so. During each period the influence of the PDO is virtually unmistakable. Also, during the early years of the past century, coastal upwelling intensified due to an intensification of the subtropical high pressure system which overlies the central North Pacific during summer [20]. However, by the early 1920s, this intensification had apparently abated leading to weaker winds along the coast and reduced coastal upwelling. Weaker coastal upwelling is, of course, consistent with increasing SSTs along the coast which is what we have observed.

2.2.2 Interannual and interdecadal variabilities

As we have stated, based on the long-term trends inside and outside Monterey Bay, temperatures increased rapidly from 1920 through at least 1940 inside the bay. Outside the bay, temperatures continued to increase more gradually up to approximately 1960. A major El Nino occurred in 1940–1941 (**Figure 6**), and the Pacific decadal oscillation index (http://research.jsiao.washington.edu/pdo/PDO) had one of its two primary maxima during the past century circa 1940 (**Figure 12**) and, together, almost certainly contributed to these trends during this period. From the late 1940s to the late 1960s, trends inside the bay show little change, but by 1970 temperatures increase significantly up to the early 1990s, consistent with the massive El Nino episode of 1982–1983 plus a second maximum in the PDO circa 1990 (**Figure 12**). Inside the bay, by the mid-1990s, SSTs finally started to decrease, and they decreased steadily until 2014, again consistent with the strongly decreasing amplitude of the PDO during this period.

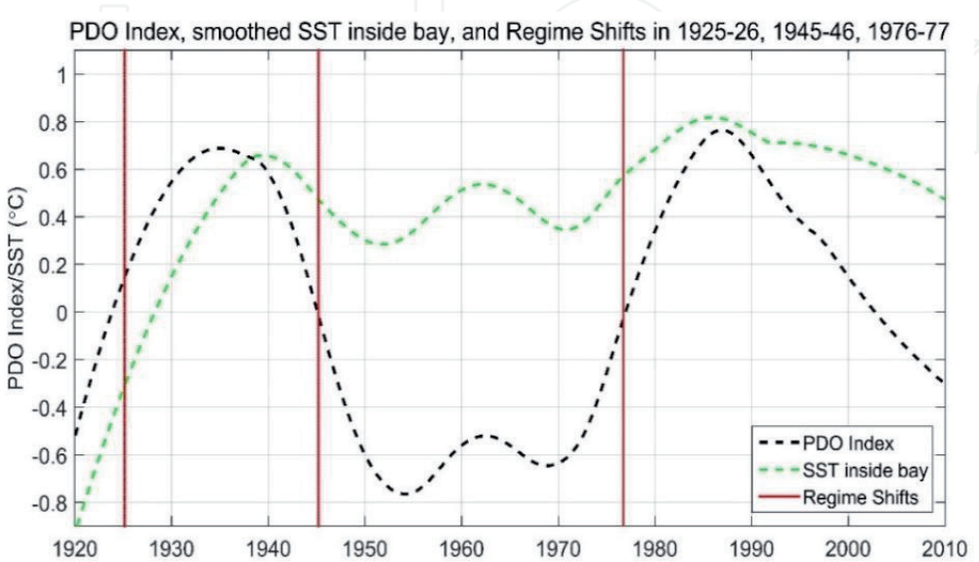

Figure 12.
A smoothed version of the Pacific decadal oscillation index (°C) is shown (dashed curve—black) together with a smoothed version of the SST record from inside the bay (dashed curve—green). Superimposed on these plots are three regime shifts that occurred during the past century (vertical red lines).

After 1960, trends outside the bay show a pattern that is in opposition to the trend inside the bay with SSTs decreasing steadily up to the early 1990s, consistent with the cooling trends observed by Garcia-Reyes and Largier [9]. By the mid-1990s, the rate of cooling increased significantly through 2013 and is likely due to the added influence of the PDO, a period where the amplitude of the PDO index likewise decreased rapidly.

2.2.3 The PDO and the impact of regime shifts

Two processes that have received considerable attention are El Nino warming events and the PDO because of their expected importance in contributing to the warming (cooling) process. The time scales of El Nino warming events off central California vary, but they last for at least 6 months and can persist for periods of up to 2 years. The El Nino episodes in 1940–1941, 1958–1959, and 1982–1983 are examples of events that lasted for almost 2 years. Although these events are transient, they may leave an imprint that is imbedded in memory of the ocean for decades [48].

The time scales of the long-term oscillations that characterize the PDO are 20–30 years [49]. However, the changes in physical properties associated with the change in phase of the PDO are far shorter. These changes, i.e., regime shifts, have time scales that are of the order of 6 months [50]. Since 1920, three major regime shifts have occurred: 1925–1926, 1945–1946, and 1976–1977. These events have each been associated with a phase change in the PDO.

Figure 12 shows a smoothed version of the PDO index together with a smoothed version of the SST data from inside the bay. We note that the events in 1925–1926 and 1976–1977 occur when the slope of the PDO index is positive, leading to changes in temperature along the California coast that were positive, whereas the event in 1945–1946 occurred when the slope of the PDO was negative [50]. In this case, the event led to a decrease in long-term temperature along the coast of California. It is important to note that although the signs of these changes along the coast of California were as indicated above, in other parts of the North Pacific, basin changes of opposite sign in SST were observed with respect to 1976–1977 event [51, 52].

We now take a closer look at these events. Because they are buried in the day-to-day natural variability of the data, they are difficult to detect and localize. Breaker [50] used cumulative sums to identify and localize regime shifts that have occurred since the early 1920s. Regime shifts produce a characteristic pattern in the cumulative sum that allows us to estimate when the event occurred, its duration, and its midpoint, t_o.

Once a regime shift has occurred, are the changes that occur short-lived or are they sustained over longer periods? To address this question, we employed a method called the expanding mean [51]. We start at the midpoint of these events and calculate the mean values proceeding forward and backward in time and then compare the results after we have proceeded in each direction for several years or longer.

Near t_o, the mean values vary widely because only a few observations enter into the calculation, but after 2–3 years, the plots generally start converging to mean values that become relatively stable. The influence of El Nino episodes was avoided wherever possible. These plots were generated for each event.

The expanding mean plot for the 1925–1926 regime shift showed that stable mean differences first appeared at 1.5–2 years out from t_o, with values in the range of +0.3°C estimated between years 2 and 3.5 in the forward direction. The differences remain consistently positive out to year 6, but a major El Nino event in 1930 precluded a more extensive comparison. The expanding mean plots for the 1945–1946 regime shift revealed that a decrease in SST did occur along the central California coast. Here, the differences are greater after 2–3 years and were

consistently negative out to 10 years. The El Nino of 1940–1941 notwithstanding, we estimate a mean decrease of at least −0.4°C. For the 1976–1977 event, from 3 to 6 years forward from t_o, the differences were consistently positive with values that ranged from about +0.1°C to almost +0.5°C. Overall, after the first ~2.5 years, positive differences between the two curves were sustained out to almost 10 years, with increases, on average, that were of the order of +0.2°C.

These results suggest that small but sustained changes in the mean value of temperature occurred following the 1925–1926, 1945–1946, and 1976–1977 regime shifts. These changes appear to have been sustained for periods of up to a decade and perhaps for the entire period between regime shifts. As a result, these events, although brief in nature, may well contribute to the long-term trends that we have sought to identify.

2.3 Discussion

The long-term trends obtained in the foregoing analyses and presented earlier were obtained using singular spectrum analysis (SSA) and ensemble empirical mode decomposition (EEMD). The results tend to be similar within each domain although significant differences arose. Based on our experience in this study and others, we favor the results obtained using EEMD for the reasons we discuss in Section 4.3.2. However, SSA provided valuable guidance in helping us decide on a suitable definition for the long-term trend.

Monthly averaged SSTs from January 1920 through December 2013 for two adjacent areas, the central California coast and Monterey Bay, have been examined for long-term trends based on the results from EEMD. These trends show that from 1920 to 1940, temperatures increased rapidly in both domains. After 1940, the trends inside and outside the bay are basically different. Inside the bay the trends indicate that temperatures tended to increase from about 1950 through 1990, while outside the bay, they decreased continuously from about 1960 through 2013. Temperatures inside the bay also decreased after 1990 until the arrival of a major thermal anomaly in 2014. Of particular note is the period during the 1970s and 1980s where trends inside the bay indicate that temperatures increased at rates higher than at any other time prior to 1940. In early 2014, a major temperature anomaly referred to as the "Blob" arrived along the central California coast that lasted for almost 2 years [1], and made it virtually impossible to continue the analysis beyond that point since our primary goal was to compare long-term trends inside Monterey Bay and outside the bay off the open coast.

Based on our nonseasonal results from EEMD, although SSTs inside the bay have decreased rapidly since the early 1990s, overall, if we consider the entire record, they have increased from about 12.6°C to almost 13.0°C over the 94 years from 1920 to 2014. Outside the bay SSTs may not have changed much over the entire 94-year period. They reached a maximum of slightly over 13.4°C circa 1960 with values of about 12.4°C in 1920 and a value of about 12.3°C at the end of 2013. For comparison, although we do not show the results from linear analyses that were performed, they indicate that the linear trend inside the bay is positive and statistically significant, whereas the trend outside the bay is negative and is not statistically significant.

To take a closer look at the data, a higher resolution analysis based on smoothing was conducted. The data were decomposed into two seasons, summer (MJJ) and winter (NDJ). Based on these decompositions (**Figure 11**), significant warming inside the bay since the 1970s has occurred only during the summer. Thus, there is most likely a connection to coastal upwelling, albeit indirect. Outside the bay, SSTs decreased continuously during this period. According to Garcia-Reyes and Largier [9], SSTs along the central California coast have decreased since the early 1980s

due to increased coastal upwelling which is directly related to increased upwelling-favorable winds. Our results are consistent with theirs where the data overlap, and so it is likely that the same processes have been at work back to at least the 1960s, and perhaps a decade or two earlier, off central California.

According to Bakun [10], the increase in coastal upwelling over the past several decades is related to increased heating in inland California and the surrounding area that has intensified the thermal low pressure system in the Southwestern United States. This intensified low pressure system together with the subtropical high pressure system off the coast of California has increased the pressure gradient between the two regions. This increase in the onshore-offshore pressure gradient in turn produces stronger winds along the California coast and thus more intense coastal upwelling. The increase in inland heating may be due to sustained climate warming or simply to long-term climate variability.

Why increased warming occurred inside the bay until ~1990, while cooling occurred continuously off the coast of central California since about 1960, is a curious fact if we assume that the behavior of bay waters is directly related to what happens further offshore. One possibility is that as coastal upwelling increased off the coast, more intense upwelling took place in the upwelling center off Point Ano Nuevo, located approximately 40 km north of Monterey Bay (**Figure 1**), whose waters are advected down the coast toward the bay. This flow is most likely a manifestation of the coastal jet which typically flows in close proximity to the coast [53]. This flow bifurcates when it reaches the bay and part flows into the bay and part flows offshore [15, 16]. If the down-coast flow increased as upwelling increased in the Ano Nuevo upwelling center, then the process of bifurcation or the location where it occurred could have been altered. Such a change might well have resulted in less upwelled water entering the bay and more going elsewhere. As a result, with less cold, upwelled water entering the bay, SSTs would have increased. In this case, the waters inside and outside the bay may still co-vary, but this co-variation could take the form of an inverse relationship rather than a direct one.

Continuing, why then did temperatures inside the bay start decreasing in the early 1990s, becoming more in line with what had been taking place outside the bay since the early 1960s? It is possible that what occurred during the 1960s inside the bay may have resulted in a basically unstable flow regime that could not be sustained indefinitely and so it eventually returned to its original state. Other possibilities exist, but this question presents an ideal opportunity to employ a hydrodynamic model of Monterey Bay and the surrounding area to address it.

To summarize the seasonal analyses, regardless of the season, there were very high rates of warming during the first 20 years of each record and only slightly less rapid rates of cooling after ~1990. The very high rates of increasing temperature are in agreement with Field et al. [20] who found that SSTs off southern California rose rapidly by the mid-1920s due to secular warming, consistent with the rapidly increasing SSTs we have observed off central California and Monterey Bay during the same period.

Before we leave the seasonal results, we point out that most of what has been said and will be said regarding the various analyses refers primarily to those results obtained from the EEMD modal decompositions, i.e., the long-term trends, and not from the seasonal analyses although these results have added additional insight at the shorter time scales.

In comparing the physical properties and flow along the central coast and Monterey Bay between November and February, i.e., during winter, waters inside and outside the bay are dominated by poleward flow associated with the Davidson Current [13]. As a result we expect that these waters tend to co-vary in unison and that the physical properties are similar. The results shown in **Figure 11b** are

consistent with this view. However, during summer the situation is very different (**Figure 11a**), and so it is not surprising that differences in the trends occur for the reasons we have just described.

A number of processes contribute to the long-term trends in SST that we have observed. Interpreting these trends in terms of the oceanic processes that contribute to them is not necessarily straightforward. However, from the modal variances obtained from our EEMD decompositions, we can identify a number of these processes and, to some degree, estimate their relative importance. We start with coastal upwelling. It is one of the dominant processes along the California coast. The first mode from each EEMD decomposition contains variability with periods that range from less than 2 months to slightly greater than 6 months. In each case it accounts for approximately 15% of the total variance. According to our results and those of Garcia-Reyes and Largier [9], coastal upwelling has continued to intensify over at least the past several decades, in agreement with Bakun [10]. Offshore, SSTs have generally decreased since as early as 1940 based on our seasonal analyses. Thus, it is clear that coastal upwelling is a major contributor to lower SSTs offshore and may have contributed indirectly to higher SSTs inside Monterey Bay.

A number of upwelling-related processes also fall within a similar range of time scales as coastal upwelling. These include offshore Ekman transport, Ekman pumping, the spring transition, and squirts and jets. Although not entirely separate from coastal upwelling, the growth and decay of cyclonic and anticyclonic eddies and the evolution of ocean fronts are included in this range. In the last case, with regard to eddies, although their life cycles often exceed 6 months, much of the variability associated with them occurs on shorter time scales.

Although the annual cycle is the major contributor to the variances in SST inside and outside the bay, they have little or no apparent impact on the long-term trends. Conversely, El Nino warming episodes and the Pacific decadal oscillation are clearly important. It is difficult to estimate the variances associated with the El Nino and the PDO separately because they occupy at least four adjacent modes in our EEMD decompositions (**Figure 6**). According to the sequences, the El Nino episodes gradually coalesce into the PDO as we progress from mode 5 to mode 8 in each case. A similar coalescence takes place inside the bay for the same modes. Together, these modes account for only ~10% of the total variance, but the processes they represent make the greatest contributions to the long-term trends because they have the longest time scales. Finally, consistent with our observations, it is now well recognized that the PDO owes its existence in large measure to the ENSO phenomenon [54–56].

Although the variance of the PDO is relatively small in each case, its influence on the long-term behavior of the data is highly significant. Of particular note, our decompositions revealed that the variance of the PDO, although relatively small compared to the other modes, is far greater inside the bay than it is outside the bay. As a result, we would expect its impact on the long-term trends to be greater inside the bay. That this is the case is clearly shown in **Figure 9** where the maximum value of the long-term trend inside the bay occurs in the early 1990s and thus coincides with one of the two major maxima in the PDO index (**Figure 12**). Why the amplitude of the PDO is greater inside the bay may be due to its containment within a limited domain where its energy tends to accumulate more rapidly than it can dissipate. If we are correct, then this relationship may hold in other coastal regions where similar embayments are found.

Unlike El Nino warming events that are intermittent in nature, the influence of the PDO, although less apparent, may be both continuous and transient. Transient influences may occur when there are phase changes in the PDO. These phase changes often correspond to regime shifts. The time scale of these events is on the order of 6 months. Our results suggest that small but sustained changes in

the mean value of temperature occurred following the 1925–1926, 1945–1946, and 1976–1977 regime shifts. These changes appear to be sustained over periods of up to a decade or longer. Also, regarding the 1976–1977 event, in two related studies, one off the coast of Hawai'i [48] in the central Pacific and the second off the coast of South Korea [49] in the western Pacific, it was found that SSTs decreased rather than increased as they had off central and southern California during the 1976–1977 event [47]. We conclude by stating that the influence of the PDO may be twofold where its total impact is composed of continuous and transient contributions.

Finally, the long-term trend in SST inside the bay departs significantly from the trend further offshore over the 94-year period from 1920 to 2014. However, the differences in these trends were far greater during the 30-year period between 1960 and 1990 which imply that significant changes in the local circulation in and around the bay must have occurred during that period. We make an important distinction, however, between the differences in the trends we have observed and the extent to which they reflect independent behavior. It is likely that during the 1970s and 1980s, for example, where the trends differ significantly, these waters still co-varied but the relationship between them was not direct but indirect as we have said before. Thus, upwelling off the coast could be increasing at roughly the same time that upwelled waters entering Monterey Bay are decreasing.

3. Conclusions

Although the results of Garcia-Reyes and Largier [9] indicate that coastal upwelling along the coast of California has intensified since the early 1980s, our results suggest that this cooling process has been at work since at least the early 1960s and possibly earlier.

Nonlinear methods were used throughout this study to estimate the long-term trends. In addition to fitting long-term variability in the data more realistically, nonlinear trends will, in most cases, have smaller confidence intervals than those associated with the corresponding linear trends. Also, of importance, the nonlinear trends often provide more insight into the processes that contribute to them.

The major thermal anomaly that occurred off the coast of central California in early 2014 made it virtually impossible to conduct a meaningful analysis of the long-term trends because of its magnitude and duration. Thus, this chapter serves as a period piece that spans a recent 94-year period during which we were able to observe and hopefully better understand the relationship between the waters of Monterey Bay and the waters further offshore along the central California coast.

We often find a sensitive interplay between resolving the trend and trying to interpret it. As the resolution is increased, new features often emerge that make it difficult to decide what part of the long-term variability contributes to the trend and what part does not. This problem was encountered in 2.1.2 of the present study.

Our results show that the amplitude of the Pacific decadal oscillation (PDO) is approximately twice as large inside Monterey Bay as it is outside the bay. This relationship most likely derives from the fact that Monterey Bay is partially enclosed. As a result, energy associated with the PDO that enters the bay may accumulate more rapidly than it can be dissipated, leading to higher amplitudes within the interior, overall. If we are correct, then we might expect to find a similar relationship in other coastal regions where embayments exist.

We conclude the warming that occurred during the first two decades of our data sets, i.e., from 1920 to 1940, was highly unusual. During this period SSTs increased at rates approaching 5°C/100 years. We know that SSTs off southern California also

experienced a rapid increase in SST by the mid-1920s [20], and that during this same period, global SSTs likewise increased significantly [57].

Using spectral decompositions of the data, we were able to illustrate over a sequence of modes the process of El Nino episodes evolving or coalescing into the Pacific decadal oscillation, consistent with recent theoretical results that emphasize the contribution that El Ninos make to the formation of the PDO [54–56].

Although it would appear that the waters inside and outside Monterey Bay often act independently, this may not be the case. We do concur that these waters, to a large extent, co-vary. The point is that apparent independence and co-variation are not mutually exclusive terms. Although we have shown at least one way in which these terms can be reconciled, other possibilities exist.

In this study we examined three regime shifts that occurred in 1925–1926, in 1945–1946, and in 1976–1977 and found that small changes in the mean temperature, of order 0.5°C or less, accompanied these events based on the data from Monterey Bay. These regime shifts coincided in each case with a phase change in the PDO. Although these changes were relatively small, they were often sustained for periods of up to a decade or longer, and this tendency may be one of their defining characteristics.

The physical behavior of regime shifts is not completely understood. However, it is becoming apparent, based on limited observations, that some regions within the Pacific basin exhibit an increase in SST, while at others, a decrease is observed during the same event, in this case, during the 1976–1977 regime shift. The spatial distribution of these changes in sign around the North Pacific also raises the possibility that what we may be observing, if we connect the dots, is a standing wave pattern. Such a standing wave would most likely have a wavelength governed by the dimensions of the basin, motion governed by the phase of the Pacific decadal oscillation, and a period of approximately 20–30 years, based on the intervals between the events we have examined. Periods in this range are in close agreement with [58] who estimated the mean interval between events to be 23 years based on the historical PDO record that dates back to 1650.

Finally, why is the work presented here of value? One reason is that by obtaining a better understanding of the relationship between bay waters and those further offshore, we are better able to predict the behavior of one system when we only have information regarding the other. In the signal processing world, such a relationship would be referred to as a transfer function.

Acknowledgements

Steve Worley and Zaihua Ji from NCAR are thanked for providing the SST data from ICOADS. Dr. Mark Denny from the Hopkins Marine Station is thanked for providing SST data adjacent to the Hopkins Marine Station for the purpose of evaluating the Hopkins SST data. David Crosby, Professor Emeritus of Statistics at American University, is thanked for suggesting the method of estimating the uncertainty associated with the trends obtained using SSA and EEMD. Finally, one anonymous reviewer is thanked for providing a number of helpful comments and suggestions for improvement that have been incorporated in the final version of the text.

Author details

Laurence C. Breaker[1,2]

1 Moss Landing Marine Laboratories, Moss Landing, CA, United States of America

2 University of Delaware, Newark, DE, United States of America

*Address all correspondence to: laurence.breaker@gmail.com

IntechOpen

References

[1] Bond NA, Cronin MF, Freeland H, Mantua N. Causes and impacts of the 2014 warm anomaly in the NE Pacific. Geophysical Research Letters. 2015;**42**:3414-3420. DOI: 10.1002/2015GL063306

[2] Lipphardt BL, Small D, Kirwan AD Jr, Wiggins S, Ide K, Grosch CE, et al. Synoptic Lagrangian maps: Application to surface transport in Monterey Bay. Journal of Marine Research. 2006;**64**:221-247. Available from: http://www.journalofmarineresearch.org

[3] Skogsberg T. Hydrography of Monterey Bay, California: Thermal conditions, 1929-1933. Transactions of the American Philosophical Society. 1936;**29**:152. Available from: https://www.amphilsoc.org/publications

[4] Skogsberg T, Phelps A. Hydrography of Monterey Bay, California: Thermal conditions, part II, 1934-1937. Transactions of the American Philosophical Society. 1946;**90**:350-386. Available from: https://www.amphilsoc.org/publications

[5] Woodson CB et al. Local diurnal upwelling driven by sea breezes in northern Monterey Bay. Continental Shelf Research. 2007;**27**:2289-2302. DOI: 10.1016/j.csr.2007.05.014

[6] Graham NE, Largier JL. Upwelling shadows as nearshore retention sites: The example of northern Monterey Bay. Continental Shelf Research. 1997;**17**:509-532. DOI: 10.1029/2009JC005623

[7] Garcia-Reyes M, Largier J. Seasonality of coastal upwelling off central and northern California: New insights including temporal and spatial variability. Journal of Geophysical Research. 2012;**117**:C12013, 15 pages. DOI: 10.1029/2011JC007629

[8] Mendelssohn R, Schwing FB. Common and uncommon trends in SST and wind stress in the California and Peru-Chile current systems. Progress in Oceanography. 2002;**53**:141-162. Available from: https://www.infona.pl/resource/bwmeta1.element.elsevier-027a36a5-dd40-39a3-a8ab-9e2456f06956/tab/citations

[9] Garcia-Reyes M, Largier J. Observations of increased wind-driven coastal upwelling off central California. Journal of Geophysical Research. 2010, 2010;**115**:C04011, 8 pages. DOI: 10.1029/2009JC005576

[10] Bakun A. Global climate change and intensification of coastal ocean upwelling. Science. 1990;**247**:198-201. DOI: 10.1126/science.247.4939.198

[11] Snyder MA, Sloan LC, Diffenbaugh NS, Bell JL. Future climate change and upwelling in the California Current. Geophysical Research Letters. 2003;**30**:1823, CLM, 8 pages. DOI: 10.1029/2003GL017647

[12] Mooers CNK, Flagg CN, Boicourt WC. Prograde and retrograde fronts. In: Oceanic Fronts in Coastal Processes. Springer-Verlag; 1978. pp. 43-58. DOI: 10.1007/978-3-642-66987-3_6

[13] Breaker LC, Broenkow WW. The circulation of Monterey Bay and related processes. Oceanography and Marine Biology. Annual Review. 1994, 1994;**32**:1-64. ISSN 0078-3218

[14] Lasker R. Food chains and fisheries: An assessment after 20 years. In: Towards a Theory on Biological-Physical Interactions in the World Ocean. Kluwer; 1988. pp. 173-182. Available from: https://link.springer.com/chapter/10.1007/978-94-009-3023-0_9

[15] Rosenfeld LK, Schwing FB, Garfield N, Tracy DE. Bifurcated flow from an upwelling center: A cold water source for Monterey Bay. Continental Shelf Research. 1994;**14**:931-964. DOI: 10.1016/0278-4343(94)90058-2

[16] Tracy DE. Source of cold water in Monterey Bay observed by AVHRR satellite imagery [thesis]. Monterey, California: Naval Postgraduate School; 1990. p. 126

[17] Barry JP, Baxter CH, Sagarin RD, Gilman SE. Climate-related, long term faunal changes in a California rocky intertidal community. Science. 1995;**267**:672-675. Available from: https://www.ncbi.nlm.nih.gov/pubmed/17745845

[18] Sagarin RD, Barry JP, Gilman SE, Baxter CH. Climate-related change in an intertidal community over short and long time scales. Ecological Monographs. 1999;**69**:465-490. Available from: http://www.bioone.org/doi/pdf/10.3398/042.007.0120

[19] Breaker LC. What's happening in Monterey Bay on seasonal to interdecadal time scales? Continental Shelf Research. 2005;**25**:1159-1193. DOI: 10.1016/j.csr.2005.01.003

[20] Field DB, Baumgartner TR, Charles C, Ferriera-Bartrina V, Ohman MD. Planktonic foraminifera of the California Current reflect twentieth century warming. Science. 2006;**311**:63-66. DOI: 10.1126/science.1116220

[21] Breaker LC, Broenkow WW, Denny MW. Reconstructing an 83-Year Time Series of Daily Sea Surface Temperature at Pacific Grove, California. Scripps Institution of Oceanography Library. Paper 7; 2006. Available from: http://repositories.cdlib.org/sio/lib/7

[22] Cleveland WS. Robust, locally weighted regression and smoothing scatterplots. Journal of the American Statistical Association. 1979;**74**:829-836. Available from: http://links.jstor.org/sici?sici=0162-1459%28197912%2974%3A368%3C829%3ARLWRAS%3E2.0.CO%3B2-L

[23] Fuller WA. Introduction to Statistical Time Series. Wiley Series on Probability and Statistics; 1996. pp. 475-476. Available from: https://www.amazon.com/Introduction-Statistical-Time-Wayne-Fuller/dp/0471552399

[24] Hamilton JD. Time Series Analysis. Princeton: Princeton University Press; 1994, First chapter. Available from: https://press.princeton.edu/links.html

[25] Jevrejeva S, Grinsted A, Moore JC, Holgate S. Nonlinear trends and multiyear cycles in sea level records. Journal of Geophysical Research. 2006;**3**:C09012. DOI: 10.1029/2005JC003229

[26] Breaker LC, Loor HR, Carroll D. Trends in sea surface temperature off the coast of Ecuador and the major processes that contribute to them. Journal of Marine Systems. 2016;**164**:151-164. DOI: 10.1016/j.jmarsys.2016.09.002

[27] Esterby SR. Review of methods for the detection and estimation of trends with emphasis on water quality applications. Hydrological Processes. 1996;**10**:127-149. DOI: 10.1002/(SICI)1099-1085(199602)10:2%3C127::AID-HYP354%3E3.0.CO;2-8

[28] Wu Z, Huang NE, Long SR, Peng C-K. On the trend, detrending, and variability of nonlinear and nonstationary time series. Proceedings of the National Academy of Sciences. 2007;**104**:14889-14894. DOI: 10.1073/pnas.0701020104

[29] Alexandrov T, Bianconcini S, Dagum EB, Maas P, McElroy T. A

review of some modern approaches to the problem of trend extraction. Econometric Reviews. 2012;**31**:593-624. Available from: http://scholar.google.de/citations?user=NUjVCEwAAAAJ&hl=de

[30] Alexandrov T. A method of trend extraction using singular spectrum analysis. Revstat—Statistical Journal. 2009;**7**:1-22. Available from: https://arxiv.org/abs/0804.3367

[31] Elsner JB, Tsonis AA. Singular Spectrum Analysis: A New Tool in Time Series Analysis. Plenum Press; 1999. pp. 51-65. DOI: 10.1007/978-3-642-34913-3

[32] Golyandina N, Nekrutkin V, Zhigljavsky A. Analysis of Time Series Structure: SSA and Related Techniques. Chapman & Hall/CRC; 2001. pp. 44-53. ISBN 1-58488- 194-1

[33] Ghil M et al. Advanced spectral methods for climatic time series. Reviews of Geophysics. 2002;**40**:1-41. DOI: 10.1029/2000RG000092

[34] Golyandina N, Zhigljavsky A. Singular Spectrum Analysis for Time Series. Springer; 2013. pp. 37-39. DOI: 10.100/978-3-642-34913-3

[35] Golyandina N, Korobeynikov A, Zhigljavsky A. Singular Spectrum Analysis with R. Springer, eBook; 2018. DOI: 10.1007/978-3-662-57380-8

[36] Wu Z, Huang NE. Ensemble empirical mode decomposition: A noise-assisted data analysis method. Advances in Adaptive Data Analysis. 2009;**1**:1-41. DOI: 10.1142/S1793536909000047

[37] Huang NE et al. The empirical mode decomposition and the Hilbert spectrum for nonlinear and non-stationary time series analysis. Proceedings of the Royal Society of London, Series A. 1998;**454**:903-995. DOI: 10.1098/rspa.1998.0193

[38] Huang NE. Introduction to Hilbert-Huang transform and some recent developments. In: The Hilbert-Huang Transform in Engineering. Taylor & Francis; 2005. pp. 1-24. ISBN-13: 978-0-8493-3422-1

[39] Huang NE. Introduction to the Hilbert-Huang transform and its related mathematical problems. In: The Hilbert-Huang Transform and its Applications. World Scientific; 2005. pp. 1-26. ISBN 981-256-376-8

[40] Huang NE, Wu Z. A review on Hilbert-Huang transform: Method and its applications to geophysical studies. Reviews of Geophysics. 2008;**46**:1-23. DOI: 10.1029/2007RG000228

[41] Vautard R, Yiou P, Ghil M. Singular spectrum analysis: A toolkit for short, noisy, chaotic signals. Physica D. 1992;**58**:95-126. DOI: 10.1016/0167-2789(92)90103-T

[42] Flandrin P, Goncalves P, Rilling G. EMD equivalent filter banks from interpretation to applications. In: The Hilbert-Huang Transform and its Applications. World Scientific; 2005. pp. 57-74. Available from: http://perso.ens-lyon.fr/patrick.flandrin/HHT05.pdf

[43] Checkley DM, Barth JA. Patterns and processes in the California Current System. Progress in Oceanography. 2009;**83**:49-64. DOI: 10.1016/j.pocean.2009.07.028

[44] Mantua N, Hare S. The Pacific decadal oscillation. Journal of Oceanography. 2002;**58**:35-44. DOI: 10.1023/A:1015820616384

[45] Mann ME. On smoothing potentially non-stationary time series. Geophysical Research Letters. 2004;**31**:L07214, 4 pages. DOI: 10.1029/2004GL019569

[46] Curry JA, Webster PJ. Climate science and the uncertainty monster.

Bulletin of the American Meteorological Society. 2011;**3139**(1):1667-1682. DOI: 10.1175/2011BAMS3139.1

[47] Moore JC, Grinsted A, Jevrejeva S. New tools for analyzing time series relationships and trends. Eos, Transactions of the American Geophysical Union. 2005;**86**:226-232. Available from: https://www.glaciology.net/publication/2005-12-24-new-tools-for-analyzing-time-series-relationships-and-trends/

[48] Fraedrich K, Blender R. Scaling of atmospheric and ocean temperature correlations in observations and climate models. Physical Review Letters. 2003, 2003;**90**:108501-1-108501-4. DOI: 10.1103/PhysRevLett.90.108501

[49] Mantua NJ, Hare SR, Zhang Z, Wallace JM, Francis RC. A Pacific interdecadal climate oscillation with impacts on salmon production. Bulletin of the American Meteorological Society. 1997;**78**:1069-1079. Available from: http://citeseerx.ist.psu.edu/viewdoc/download?doi=10.1.1.553.1185&rep=rep1&type=pdf

[50] Breaker LC. A closer look at regime shifts based on coastal observations along the eastern boundary of the North Pacific. Continental Shelf Research. 2007;**27**:2250-2277. DOI: 10.1016/j.csr.2007.05.018

[51] Breaker LC, Flora SJ. Expressions of the 1976-77 and 1988-89 regime shifts in sea surface temperature off southern California and Hawai'i. Pacific Science. 2009;**63**:39-60. Available from: https://scripps.ucsd.edu/programs/shorestations/publications/

[52] Jo Y-H, Breaker LC, Tseng Y-H, Yeh S-W. A temporal multiscale analysis of the waters off the east coast of South Korea over the past four decades. Terrestrial, Atmospheric and Oceanic Sciences. 2014;**25**:415-434. DOI: 10.3319/TAO.2013.12.31.01

[53] Hickey BM. Then California Current System—Hypotheses and facts. Progress in Oceanography. 1979;**8**:191-279. DOI: 10.1016/0079-6611(79)90002-8

[54] Newman M, Gilbert GP, Alexander MA. ENSO-forced variability of the Pacific decadal oscillation. Journal of Climate. 2003;**16**:3853-3857. Available from: http://citeseerx.ist.psu.edu/viewdoc/download?doi=10.1.1.477.8989&rep=rep1&type=pdf

[55] Schneider N, Cornuelle BD. The forcing of the Pacific decadal oscillation. Journal of Climate. 2005;**18**:4355-4373. DOI: 10.1175/JCLI3527.1

[56] Shakun JD, Shaman J. Tropical origins of North and South Pacific decadal variability. Geophysical Research Letters. 2009;**36**:L19711, 5 pages. DOI: 10.1029/2009GL040313

[57] Enfield DB, Mestas-Nunez AM. Interannual to multidecadal climate variability and its relationship to global sea surface temperatures. In: Inter-Hemispheric Climate Linkages. Academic Press; 2001. pp. 17-29. ISBN: 9780124726703

[58] Gedalof Z, Smith DJ. Interdecadal climate variability and regime-scale shifts in Pacific North America. Geophysical Research Letters. 2001;**28**:1515-1518. Available from: https://www.uoguelph.ca/cedar/Pubs/gedalof_and_smith_GRL.pdf